Scalable Spin Squeezing in Two-Dimensional Arrays of Dipolar Large-S Spins

Youssef Trifa and Tommaso Roscilde
ENS de Lyon, CNRS, Laboratoire de Physique, F-69342 Lyon, France

(Received 25 September 2023; accepted 16 July 2024; published 19 August 2024)

We theoretically show that the spin-spin interactions realized in two-dimensional Mott insulators of large-spin magnetic atoms (such as Cr, Er, or Dy) lead to scalable spin squeezing along the nonequilibrium unitary evolution initialized in a coherent spin state. An experimentally relevant perturbation to the collective squeezing dynamics is offered by a quadratic Zeeman shift, which leads instead to squeezing of individual spins. Making use of a truncated cumulant expansion for the quantum fluctuations of the spin array, we show that, for sufficiently small quadratic shifts, the spin squeezing dynamics is akin to that produced by the paradigmatic one-axis-twisting model—as expected from an effective separation between collective-spin and spin-wave variables. Scalable spin squeezing is shown to be protected by the robustness of long-range ferromagnetic order to quadratic shifts in the equilibrium phase diagram of the system that we reconstruct via quantum Monte Carlo and mean-field theory.

DOI: 10.1103/PhysRevLett.133.083601

Introduction—The controlled production and certification of many-body entangled states [1–5] is one of the most promising potentials of current quantum devices, based on quantum circuits or ultracold atoms [6–12]. Most of the present platforms realize ensembles of interacting qubits, i.e., $S = 1/2$ spin systems, which can implement universal models of quantum computation [13]. Yet working directly with *qudits* [14], i.e., elementary degrees of freedom with a higher-dimensional Hilbert space, offers several advantages, both fundamental as well as practical. Systems of qudits are realized in experiments using, e.g., photonic platforms [15], molecular magnets [16], and ensembles of large-S magnetic atoms [12]. N qudits can encode an exponentially larger amount of quantum information than N qubits; entangled states of qudits can be more resilient to noise than entangled states of qubits [15]; and using qudits as quantum sensors [4] instead of qubits can be very advantageous, in that single qudits already possess highly nonclassical states with increased sensitivity to unitary transformations. The latter aspect also hints at a very intriguing competition that qudit systems (unlike qubit ones) can exhibit between single-qudit nonclassical states and many-qudit nonclassical (i.e., entangled) states. This competition will be a central aspect of the present work.

The focus of our work is the production of entangled many-qudit states in ensembles of large-S magnetic atoms. Relevant examples—that will be discussed later—include ^{52}Cr atoms ($S = 3$), ^{168}Er atoms ($S = 6$) and ^{162}Dy atoms ($S = 8$), whose spin degrees of freedom have been manipulated in a variety of recent experiments [17–25]. When the atoms form a Mott insulator with one atom per lattice site, their large spins interact at a distance via the dipolar interaction, whose Hamiltonian (in the rotating frame of an applied large Zeeman field) reads [12,18,22]

$$\hat{\mathcal{H}} = J\sum_{i<j} D_{ij}\left[-\frac{1}{2}\left(\hat{S}_i^x\hat{S}_j^x + \hat{S}_i^y\hat{S}_j^y\right) + \hat{S}_i^z\hat{S}_j^z\right] + B_q\sum_i (\hat{S}_i^z)^2, \tag{1}$$

where $\sum_{i<j}$ runs over pairs of lattice sites, $\hat{S}_i^\mu$ ($\mu = x, y, z$) are spin-S operators, J is the overall strength of the dipolar interaction, and B_q is a quadratic Zeeman shift, originating both from the applied Zeeman field as well as from a tensorial light shift [22,23]. In the following we shall consider a square-lattice geometry (with periodic boundary conditions) for which one can have $D_{ij} = 1/r_{ij}^3$ when the applied Zeeman field, defining the quantization axis z, is perpendicular to the plane. Recent experimental studies on dipolar atoms and molecules detected the appearance of correlations induced by the dipolar interactions [20,26], but they have not yet certified entanglement. In this work we show that the dynamics of two-dimensional arrays of large-S dipolar spins, initialized in a spin-coherent state in the xy plane and governed by the Hamiltonian Eq. (1), can produce massive multipartite entanglement in the form of spin squeezing which is scalable, i.e., stronger the larger the number of atoms, following the paradigm of the one-axis-twisting (OAT) dynamics [27].

The collective OAT-like dynamics is robust to moderate values of the quadratic Zeeman shift B_q, since the evolution develops long-range correlations in the xy plane protecting the collective-spin length. At larger values of B_q long-range order still persists in the thermalized state, but the total spin length is strongly reduced, altering significantly the squeezing dynamics with respect to the OAT picture, and leading to the disappearance of squeezing for realistic system sizes. The above results stem from a combination of different

techniques for the study of the quantum dynamics, including a truncated-cumulant expansion of the quantum fluctuations in the evolved quantum state; a recently introduced approximation based on rotor/spin-wave separation; and the reconstruction of the equilibrium phase diagram of the system. Our results pave the way for the use of large-spin dipolar arrays to produce metrologically useful, multipartite entangled states.

Spin squeezing and entanglement; squeezing dynamics from RSW separation—The paradigmatic example of many-body dynamics giving rise to scalable squeezing is offered by the one-axis-twisting (OAT) model, whose Hamiltonian is that of a planar rotor whose angular momentum along the z axis is given by the collective spin, namely, $\hat{\mathcal{H}}_{\rm OAT} = (\hat{J}^z)^2/(2I)$. Here we have introduced the collective spin operator $\hat{\boldsymbol{J}} = \sum_{i=1}^{N} \hat{\boldsymbol{S}}_i$ for the ensemble of N quantum spins; and $I \sim \mathcal{O}(N)$ is the extensive moment of inertia of the rotor. When the system of N spins of length S is initialized in a coherent spin state (CSS) along x, $|\mathrm{CSS}_x\rangle = |S;x\rangle^{\otimes N}$ (where $\hat{S}^x|S;x\rangle = S|S;x\rangle$), the collective spin is of maximal length $\hat{\boldsymbol{J}}^2 = J_{\max}(J_{\max}+1)$ with $J_{\max} = NS$. The Hamiltonian evolution governed by $\mathcal{H}_{\rm OAT}$ remains in the $J_{\max}$ sector, and it produces squeezing of the collective spin, captured by the squeezing parameter $\xi_R^2 = [2NS\mathrm{Var}(\hat{J}^{\min})/\langle \hat{J}^x\rangle^2]$ where $\mathrm{Var}(\hat{J}^{\min})$ is the minimal variance of the collective spin components in the yz plane. The initial CSS has $\xi_R^2 = 1$, while $\xi_R^2 < 1$ indicates squeezing of the uncertainty along one direction in the yz plane with respect to this reference state. The OAT dynamics is known to produce an optimal squeezing $(\xi_R^2)_{\min} \sim (2NS)^{-2/3}$ at a time $t_{\min} \sim S^{-2/3}N^{1/3}$. Yet, for $S > 1/2$ the condition $\xi_R^2 < 1$ can also be satisfied at the level of individual spins—as e.g., generated by a collection of single-spin OAT models, $\hat{\mathcal{H}}_{\rm 1s-OAT} = B_q \sum_i (\hat{S}_i^z)^2$. Therefore spin squeezing *per se* is not necessarily a witness of entanglement. Yet the minimal squeezing parameter for uncorrelated S spins is $(\xi_R^2)_{\rm SQL} = (1+S)^{-1}$ (for $S > 1/2$) [4], corresponding to the standard quantum limit (SQL) for large-S spins. Hence the condition $\xi_R^2 < (1+S)^{-1}$ certifies the presence of entanglement; and the stronger condition $\xi_R^2 < [(1+kS)]^{-1}$ signals $(k+1)$-partite entanglement.

The OAT model offers an important paradigm for the squeezing dynamics of dipolar Hamiltonians in $2d$ such as Eq. (1) [28–32]. Indeed, under dipolar dynamics the collective spin length $\hat{\boldsymbol{J}}^2$, albeit not conserved, may only decrease moderately with respect to its maximum value. This property justifies a scenario of rotor/spin-wave (RSW) separation, as proposed in Refs. [33,34]. In a nutshell, the dipolar Hamiltonian, when projected onto the $J_{\max}$ sector of symmetric states, takes the form of a OAT Hamiltonian with effective moment of inertia $1/(2I) = (J/2N^2)\sum_{i\neq j} D_{ij} + (B_q/N)$, which would govern the dynamics if it remained confined to the $J_{\max}$ sector. Leakage out of this sector can be accounted for by the production of spin-wave excitations, described as finite-momentum Holstein-Primakoff (HP) bosons. If such bosons form a dilute gas, they can be described as a system of free quasiparticles, effectively decoupled from the collective spin projected on the $J_{\max}$ sector (hereafter called rotor). The dynamics of the system can therefore be cast as the independent dynamics of a rotor variable $\hat{\boldsymbol{K}}$ of length $K = J_{\max}$, governed by the OAT Hamiltonian $\hat{\mathcal{H}}_R = (\hat{K}^z)^2/(2I)$; and of linearized spin waves (SWs) at finite momentum, with Hamiltonian $\hat{\mathcal{H}}_{\rm sw} = \sum_{\boldsymbol{k}\neq 0}(\hat{b}_{\boldsymbol{k}}^\dagger, \hat{b}_{-\boldsymbol{k}})h_{\boldsymbol{k}}(\hat{b}_{\boldsymbol{k}}, \hat{b}_{-\boldsymbol{k}}^\dagger)^T$, where $h_{\boldsymbol{k}}$ is a 2×2 matrix and $\hat{b}_{\boldsymbol{k}}$ are HP boson operators (see Supplemental Material [35] for further details). Within RSW theory [33,34], the squeezing parameter is expressed as $\xi_R^2 \approx (2NS)\mathrm{Var}(K^{\min})/(\langle \hat{K}^x\rangle - N_{\rm bos})^2$, where $N_{\rm bos} = \sum_{\boldsymbol{k}\neq 0}\langle \hat{b}_{\boldsymbol{k}}^\dagger \hat{b}_{\boldsymbol{k}}\rangle$ is the population of HP bosons, renormalizing the polarization of the collective spin. Hence the squeezing dynamics of the system is akin to that of the OAT model so long as $N_{\rm bos}$ remains a small correction to the rotor magnetization up to the time $t_{\min}$. The SW dynamics develops instabilities (i.e., imaginary frequencies) for negative values of B_q (see Supplemental Material [35]), due to a ground-state transition occurring for $B_q \lesssim -J$ (for all the values of S we explored)—see further details below. Therefore we shall focus on $B_q > 0$ in the following.

OAT-like regime and its breakdown—Figures 1(a)–1(c) shows indeed that, for sufficiently small and positive B_q values, the picture offered by RSW theory applies to the dynamics generated by the Hamiltonian Eq. (1). The predictions of RSW theory are indeed found to only moderately deviate from those of a pure-rotor dynamics, for a B_q range that grows with the spin length S. This means that SWs are dilute, justifying the separation of variables. Most importantly, at short times, the RSW predictions are corroborated by a completely alternative approach based on a truncated cumulant expansion (TCE)—up to 2nd order cumulants—for the multivariate quantum fluctuations of the spin ensemble. This represents our most stringent test of the RSW predictions. The TCE approach (described in detail in the Supplemental Material [35]) is a variant of similar approaches developed for quantum many-body systems and in quantum optics [39–43]; the specificity of our formulation for large-S systems is that it can describe exactly the physics at the single-spin level, in spite of the large local Hilbert space—a trait that is essential when single-spin physics competes with many-body physics. The assumption of truncation of the cumulant hierarchy leads to unphysical results after a given time, restricting this approach to short times when strong squeezing appears, driven by the many-body physics.

An extensive comparison of the predictions of the RSW and TCE approaches for the scaling of squeezing is offered in Figs. 1(d)–1(f). There we plot the value of the squeezing

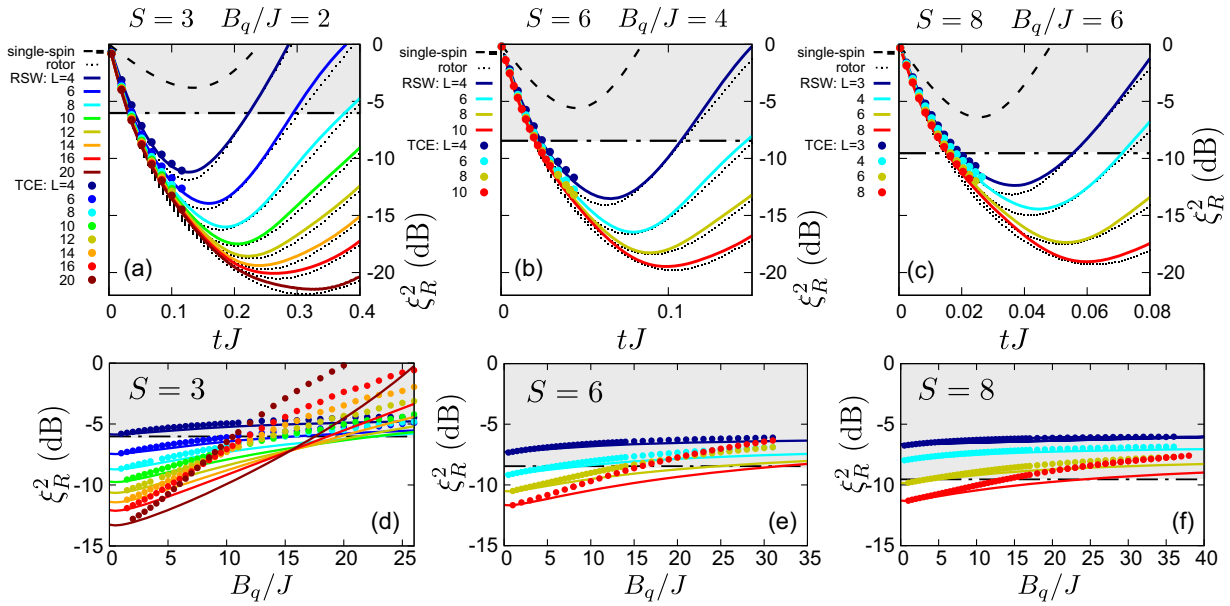

FIG. 1. Scalable spin squeezing in dipolar large-S arrays. (a)–(c) Time evolution of the squeezing parameter for various system sizes and $S = 3$, $B_q/J = 2$ (a), $S = 6$, $B_q/J = 4$ (b), and $S = 8$, $B_q/J = 6$ (a). Each panel shows the comparison between the single-spin limit; the rotor dynamics with effective moment of inertia $1/(2I)$ (see main text); the rotor/spin-wave theory (RSW) and the truncated cumulant expansion. The shaded region marks the regime $\xi_R^2 \geq (1+S)^{-1}$, in which squeezing does not witness entanglement. (d)–(f) Squeezing parameter at the time $0.3t_{\min}$ (see main text) for various system sizes as a function of B_q/J for $S = 3$ (d), $S = 6$ (e), and $S = 8$ (f). Significance of symbols in panels (d),(e), and (f) is the same as in panels (a),(b), and (c), respectively.

parameter at an earlier time with respect to the optimal squeezing one $t_{\min}$, due to the breakdown of the TCE approach mentioned above. We choose the time of observation as $0.3t_{\min}$, where $t_{\min}$ is the time at which the OAT model with coupling constant $1/(2I)$ reaches its minimum squeezing. Scalable squeezing is expected in the OAT model at this earlier time as well, albeit with a slower scaling than at $t_{\min}$ (see Supplemental Material [35]). As one can see, RSW and TCE results agree well for all system sizes over the ranges $B_q \lesssim 2J$ for $S = 3$; $B_q \lesssim 5J$ for $S = 6$; and $B_q \lesssim 7J$ for $S = 8$. These ranges correspond therefore to OAT-like scalable squeezing. For larger B_q values, the two theories (TCE and RSW) start to deviate, signaling that the picture of separation of variables underlying RSW theory breaks down. Nonetheless, as we shall also discuss in the next section, squeezing appears to remain scalable for a larger range of B_q values, but following a behavior which can no longer be understood starting from the OAT paradigm.

Scalable vs nonscalable spin squeezing, and relationship to thermodynamics—To understand the evolution in the scaling of the squeezing parameter upon increasing B_q, it is useful to consider the limit $B_q \gg J$, in which the dynamics is dominated by the quadratic Zeeman shift. In this limit (denoted by the dashed curves in Figs. 1 and 2) each spin behaves as a OAT model, exhibiting a fast depolarization

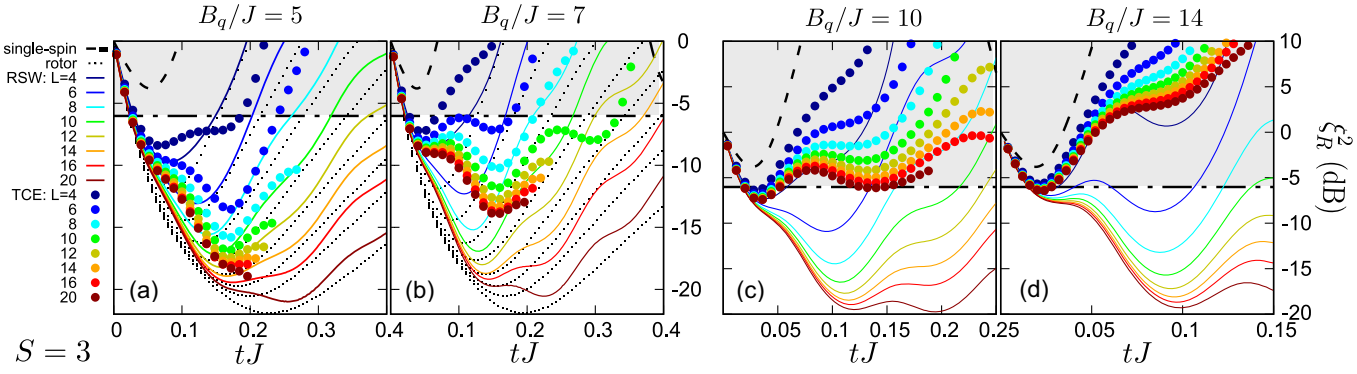

FIG. 2. Squeezing dynamics at large B_q. Time evolution of the spin squeezing parameter for $S = 3$ and three values of $B_q/J =$ (a) 5, (b) 7, (c) 10, and (d) 14. All symbols are as in Fig. 1(a).

over a time $\sim B_q\sqrt{S}$ which is system-size independent—this is the dynamics realized in recent experiments on single Dy atoms [23]. How is this single-spin dynamics connected with the collective-squeezing dynamics at small B_q? Figure 2 shows that when leaving the OAT-like regime, scalable squeezing persists, albeit with very large fluctuations in time. For sufficiently small B_q these fluctuations are partly reproduced by RSW theory [Fig. 2(a)], which attributes them to SWs—although the proliferation of finite-momentum SWs leads to the breakdown of the separation-of-variable assumption underlying RSW theory [35]. As B_q increases, the competition between single-spin and many-body physics becomes manifest [see, e.g., Figs. 2(c) and 2(d)]: under the effect of the B_q term, at short time ξ_R^2 reaches a nearly size-independent first minimum, followed by antisqueezing dynamics (i.e., ξ_R^2 increases). At later times, at least for the largest system sizes, antisqueezing stops, and ξ_R^2 begins to decrease again developing a second minimum, deeper the larger the size. This later dynamics is clearly the result of many-body physics—as revealed by its scaling nature—and it can be understood in relationship to a fundamental trait of dipolar spins in two dimensions, namely, their ability to develop long-range order at low energy [44].

At this point it is instructive to inspect the equilibrium phase diagram of the dipolar large-S Hamiltonian Eq. (1) in two dimensions, which we have reconstructed in the temperature-vs-B_q plane using numerically exact quantum Monte Carlo, as well as mean-field theory. The results are shown in Fig. 3 for the case $S = 3$ (see Supplemental Material [35] for analogous phase diagrams for $S = 6$ and 8, and details about the calculations). For a large B_q region,

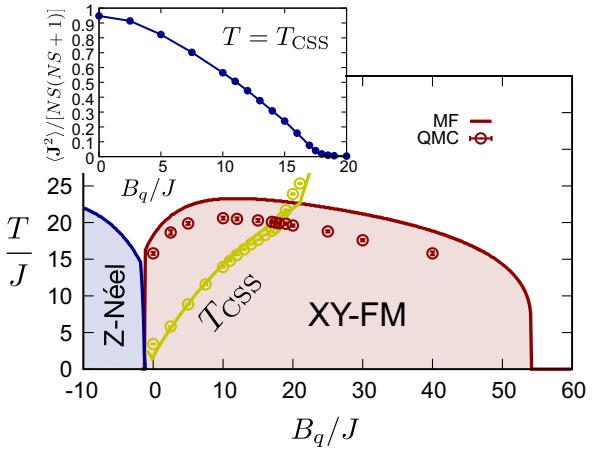

FIG. 3. Equilibrium phase diagram of the $S = 3$ dipolar XXZ model on the square lattice. The diagram shows the mean-field (MF) and quantum Monte Carlo (QMC) estimates of the transition temperature to xy ferromagnetism (XY-FM), to Néel antiferromagnetism (Z-Néel), and of the coherent-state temperature $T_{\rm CSS}$. Inset: collective-spin square modulus $\langle \hat{\boldsymbol{J}}^2\rangle$ along the $(B_q, T_{\rm CSS}(B_q))$ line, evaluated for a system of $N = 48 \times 48$ spins.

$0 \lesssim B_q \lesssim 54J$, the thermodynamics exhibits long-range ferromagnetism in the xy plane up to finite critical temperature T_c; while for $B_q \lesssim -1.1J$ the system exhibits long-range Néel antiferromagnetism along the z axis. When initialized in the CSS, the unitary evolution driven by the (nonintegrable) Hamiltonian Eq. (1) at long times is expected to thermalize the state of the system [45], so that the time average of local observables reproduce their equilibrium expectation values (denoted by $\langle \ldots \rangle_{T_{\rm CSS}}$) at a temperature $T_{\rm CSS}$ such that $\langle {\rm CSS}_x|\hat{\mathcal{H}}|{\rm CSS}_x\rangle = \langle \hat{\mathcal{H}}\rangle_{T_{\rm CSS}}$ [46]. The unitary evolution at long times is therefore sensitive to the equilibrium behavior along the $T_{\rm CSS}(B_q)$ line in the phase diagram (see Fig. 3) where the state goes from xy ferromagnetic to paramagnetic for $B_{q,c} \approx 18J$. In particular, this transition is marked by a drop of the collective spin length $\langle \hat{\boldsymbol{J}}^2\rangle$ from macroscopic values $[\sim O(N^2)]$ to microscopic ones $[\sim O(N)]$—see inset of Fig. 3.

Spontaneous breaking of the U(1) symmetry of Eq. (1) in the thermodynamic limit can have important consequences on the squeezing dynamics [31]: indeed it implies that, on finite system sizes, the initial polarization $\langle \hat{J}^x\rangle$ associated with the CSS persists for increasingly long times the larger the system size (and never vanishes in the thermodynamic limit). This is shown by our data (see Supplemental Material [35]), and was also observed experimentally in dipolar qubits [32]. As a consequence, in spite of the depolarizing effect coming from the B_q term, ferromagnetism can protect the spin-squeezing parameter from blowing up, because it prevents the denominator in the expression of ξ_R^2 from vanishing rapidly; and it can delay or even reverse the antisqueezing dynamics. Moreover the collective spin remains of macroscopic length, as guaranteed by the fact that $\langle \hat{\boldsymbol{J}}^2\rangle \sim O(N^2)$ throughout the evolution —although it may depart significantly from its (initial) maximum value $NS(NS+1)$, as shown in Fig. 3.

In spite of long-range ordering, the fast depolarization imposed by the B_q term can push the squeezing parameter to values ξ_R^2, which are systematically higher than the entanglement threshold $\xi_R^2 = (1+S)^{-1}$ (for $B_q \gtrsim 10J$), or even higher than the proper squeezing threshold $\xi_R^2 = 1$ (for $B_q/J \gtrsim 13J$ [35]). This is clearly observed in Figs. 2(c) and 2(d) (see also the Supplemental Material [35] for further data), for the system sizes we explored (up to $N = 400$ for $S = 3$). Hence collective spin squeezing—namely squeezing exceeding what can be achieved with single spins—can be lost for B_q values well below $B_{q,c}$. This situation may coexist with a persistent scaling of the squeezing parameter to lower values—namely, with persistent scalable squeezing; but extremely large system sizes, beyond the reach of current experimental setups, may be required to bring ξ_R^2 to values which are compatible with entanglement, and which therefore offer many-body metrological advantages compared to single spins (see

Ref. [23]). Long-range ferromagnetism in the thermalized state is only a necessary condition for scalable squeezing [47]; indeed scalable squeezing requires as well that $\mathrm{Var}(\hat{J}^{\mathrm{min}})/N$ scales to ever lower values with increasing size. Such a behavior is apparent in our data [35], and even persisting for $B_q > B_{q.c}$, although a power-law decay of $\mathrm{Var}(\hat{J}^{\mathrm{min}})/N$ with N is not revealed by our results. Therefore our results are not inconsistent with the conjecture of Ref. [31] that scalable squeezing persists up to the transition in the thermalized state; yet, for the system sizes we explored, the scaling behavior close to the transition appears to be very different from (and much slower than) that of the OAT model.

Conclusions—In this work we have shown that the nonequilibrium dynamics of 2D arrays of dipolar large-S spins, initialized in a coherent spin state, features multipartite entanglement in the form of scalable spin squeezing. For a sufficiently small quadratic Zeeman shift, squeezing follows the scaling of the one-axis-twisting model, in agreement with a scenario of separation of variables between collective-spin and spin-wave degrees of freedom. Our results point at the crucial role played by the quadratic Zeeman shift on the squeezing dynamics of large-S spins—and, more generally, at the competition between single-qudit vs many-qudit Hamiltonian in the entangling dynamics of qudit ensembles. To achieve collective spin squeezing in 2D dipolar arrays, the quadratic Zeeman shift should be controlled at the level of $\sim 10J$ via magnetic fields and tensor light shifts [22,23]. The two-dimensional geometries we explored in this work are essential for spin-squeezing dynamics to occur: indeed, due to its angular dependence the dipolar interaction averages to zero in three dimensions, so that the collective-spin dynamics is suppressed in three dimensions. Nonetheless purely 2D arrays of atoms can be realized either by loading a single layer in a three-dimensional optical lattice, or by trapping in quantum-gas-microscope setups, as recently demonstrated for Er [48] (see also [49,50] for recent Dy experiments). Hence our work paves the way for the realization of scalable multipartite entanglement in arrays of magnetic atoms (Cr, Er, or Dy), representing a most promising platform to realize quantum simulation and quantum information processing with ensembles of qudits.

Acknowledgments—This work is supported by ANR (EELS project) and QuantERA (MAQS project). Fruitful discussions with M. Block, N. Defenu, B. Laburthe, L. Vernac, N. Yao, and B. Ye are gratefully acknowledged. All numerical simulations have been performed on the PSMN cluster at the ENS of Lyon.

[1] R. Horodecki, P. Horodecki, M. Horodecki, and K. Horodecki, Rev. Mod. Phys. **81**, 865 (2009).
[2] O. Gühne and G. Tóth, Phys. Rep. **474**, 1 (2009).
[3] G. Tóth and I. Apellaniz, J. Phys. A **47**, 424006 (2014).
[4] L. Pezzè, A. Smerzi, M. K. Oberthaler, R. Schmied, and P. Treutlein, Rev. Mod. Phys. **90**, 035005 (2018).
[5] N. Friis, G. Vitagliano, M. Malik, and M. Huber, Nat. Rev. Phys. **1**, 72 (2019).
[6] J. García-Ripoll, *Quantum Information and Quantum Optics with Superconducting Circuits* (Cambridge University Press, Cambridge, England, 2022).
[7] C. Gross and I. Bloch, Science **357**, 995 (2017).
[8] A. Browaeys and T. Lahaye, Nat. Phys. **16**, 132 (2020).
[9] F. Schäfer, T. Fukuhara, S. Sugawa, Y. Takasu, and Y. Takahashi, Nat. Rev. Phys. **2**, 411 (2020).
[10] C. Monroe, W. C. Campbell, L.-M. Duan, Z.-X. Gong, A. V. Gorshkov, P. W. Hess, R. Islam, K. Kim, N. M. Linke, G. Pagano *et al.*, Rev. Mod. Phys. **93**, 025001 (2021).
[11] A. Kaufman and K.-K. Ni, Nat. Phys. **17**, 1324 (2021).
[12] L. Chomaz, I. Ferrier-Barbut, F. Ferlaino, B. Laburthe-Tolra, B. L. Lev, and T. Pfau, Rep. Prog. Phys. **86**, 026401 (2022).
[13] M. A. Nielsen and I. L. Chuang, *Quantum Computation and Quantum Information* (Cambridge University Press, Cambridge, England, 2010).
[14] Y. Wang, Z. Hu, B. C. Sanders, and S. Kais, Front. Phys. **8**, 589504 (2020).
[15] M. Erhard, M. Krenn, and A. Zeilinger, Nat. Rev. Phys. **2**, 365 (2020).
[16] E. Moreno-Pineda, C. Godfrin, F. Balestro, W. Wernsdorfer, and M. Ruben, Chem. Soc. Rev. **47**, 501 (2018).
[17] A. de Paz, A. Sharma, A. Chotia, E. Maréchal, J. H. Huckans, P. Pedri, L. Santos, O. Gorceix, L. Vernac, and B. Laburthe-Tolra, Phys. Rev. Lett. **111**, 185305 (2013).
[18] S. Lepoutre, J. Schachenmayer, L. Gabardos, B. Zhu, B. Naylor, E. Maréchal, O. Gorceix, A. M. Rey, L. Vernac, and B. Laburthe-Tolra, Nat. Commun. **10**, 1714 (2019).
[19] L. Gabardos, B. Zhu, S. Lepoutre, A. M. Rey, B. Laburthe-Tolra, and L. Vernac, Phys. Rev. Lett. **125**, 143401 (2020).
[20] Y. A. Alaoui, B. Zhu, S. R. Muleady, W. Dubosclard, T. Roscilde, A. M. Rey, B. Laburthe-Tolra, and L. Vernac, Phys. Rev. Lett. **129**, 023401 (2022).
[21] Y. A. Alaoui, S. R. Muleady, E. Chaparro, Y. Trifa, A. M. Rey, T. Roscilde, B. Laburthe-Tolra, and L. Vernac, arXiv:2404.10531.
[22] A. Patscheider, B. Zhu, L. Chomaz, D. Petter, S. Baier, A.-M. Rey, F. Ferlaino, and M. J. Mark, Phys. Rev. Res. **2**, 023050 (2020).
[23] T. Chalopin, C. Bouazza, A. Evrard, V. Makhalov, D. Dreon, J. Dalibard, L. A. Sidorenkov, and S. Nascimbene, Nat. Commun. **9**, 4955 (2018).
[24] A. Evrard, V. Makhalov, T. Chalopin, L. A. Sidorenkov, J. Dalibard, R. Lopes, and S. Nascimbene, Phys. Rev. Lett. **122**, 173601 (2019).
[25] T. Satoor, A. Fabre, J.-B. Bouhiron, A. Evrard, R. Lopes, and S. Nascimbene, Phys. Rev. Res. **3**, 043001 (2021).
[26] L. Christakis, J. S. Rosenberg, R. Raj, S. Chi, A. Morningstar, D. A. Huse, Z. Z. Yan, and W. S. Bakr, Nature (London) **614**, 64 (2023).
[27] M. Kitagawa and M. Ueda, Phys. Rev. A **47**, 5138 (1993).
[28] M. A. Perlin, C. Qu, and A. M. Rey, Phys. Rev. Lett. **125**, 223401 (2020).

[29] T. Comparin, F. Mezzacapo, M. Robert-de Saint-Vincent, and T. Roscilde, Phys. Rev. Lett. **129**, 113201 (2022).
[30] T. Comparin, F. Mezzacapo, and T. Roscilde, Phys. Rev. Lett. **129**, 150503 (2022).
[31] M. Block, B. Ye, B. Roberts, S. Chern, W. Wu, Z. Wang, L. Pollet, E. J. Davis, B. I. Halperin, and N. Y. Yao, arXiv:2301.09636.
[32] G. Bornet, G. Emperauger, C. Chen, B. Ye, M. Block, M. Bintz, J. A. Boyd, D. Barredo, T. Comparin, F. Mezzacapo *et al.*, arXiv:2303.08053.
[33] T. Roscilde, T. Comparin, and F. Mezzacapo, Phys. Rev. Lett. **131**, 160403 (2023).
[34] T. Roscilde, T. Comparin, and F. Mezzacapo, Phys. Rev. B **108**, 155130 (2023).
[35] See Supplemental Material at http://link.aps.org/supplemental/10.1103/PhysRevLett.133.083601 for details about (1) rotor/spin-wave theory for large-S spins; (2) the truncated-cumulant-expansion approach; (3) the scaling of the squeezing parameter at times earlier than the optimal one in the OAT dynamics; (4) extended data for the squeezing dynamics close to the thermodynamic transition; (5) equilibrium phase diagrams from quantum Monte Carlo and mean-field theory. The Supplemental Material includes Refs. [36–38].
[36] O. F. Syljuåsen and A. W. Sandvik, Phys. Rev. E **66**, 046701 (2002).
[37] F. Alet, S. Wessel, and M. Troyer, Phys. Rev. E **71**, 036706 (2005).
[38] N. Defenu, T. Donner, T. Macrì, G. Pagano, S. Ruffo, and A. Trombettoni, Rev. Mod. Phys. **95**, 035002 (2023).
[39] R. Schack and A. Schenzle, Phys. Rev. A **41**, 3847 (1990).
[40] H. A. M. Leymann, A. Foerster, and J. Wiersig, Phys. Rev. B **89**, 085308 (2014).
[41] D. Plankensteiner, C. Hotter, and H. Ritsch, Quantum **6**, 617 (2022).
[42] V. E. Colussi, H. Kurkjian, M. Van Regemortel, S. Musolino, J. van de Kraats, M. Wouters, and S. J. J. M. F. Kokkelmans, Phys. Rev. A **102**, 063314 (2020).
[43] W. Verstraelen, D. Huybrechts, T. Roscilde, and M. Wouters, PRX Quantum **4**, 030304 (2023).
[44] D. Peter, S. Müller, S. Wessel, and H. P. Büchler, Phys. Rev. Lett. **109**, 025303 (2012).
[45] Even though the thermalization process can be highly nonstandard, with the appearance of highly nonthermal states such as Schrödinger's cat states, as highlighted in Ref. [30].
[46] L. D'Alessio, Y. Kafri, A. Polkovnikov, and M. Rigol, Adv. Phys. **65**, 239 (2016).
[47] Indeed scalable squeezing is not present in the thermalized state at any finite temperature [29].
[48] L. Su, A. Douglas, M. Szurek, R. Groth, S. F. Ozturk, A. Krahn, A. H. Hébert, G. A. Phelps, S. Ebadi, S. Dickerson *et al.*, Nature (London) **622**, 724 (2023).
[49] M. Sohmen, M. J. Mark, M. Greiner, and F. Ferlaino, SciPost Phys. **15**, 182 (2023).
[50] G. Anich, R. Grimm, and E. Kirilov, arXiv:2304.12844.